Empirical prediction for travel distance of channelized rock avalanches in the Wenchuan earthquake area

Weiwei Zhan, Xuanmei Fan, Runqiu Huang, Xiangjun Pei, Qiang Xu, Weile Li

State Key Laboratory of Geohazard Prevention and Geoenvironment Protection, Chengdu University of Technology, Chengdu, 610059, China

Correspondence to: Xuanmei Fan (fxm_cdut@qq.com)

Abstract. Rock avalanches are extremely rapid, massive flow-like movements of fragmented rock. The travel path of the rock avalanches may be confined by channels in some cases, which were named as the channelized rock avalanches. Channelized rock avalanches are potentially dangerous due to their hardly predictable travel distance. In this study, we constructed a dataset with detailed characteristic parameters of 38 channelized rock avalanches triggered by the 2008 Wenchuan earthquake using the visual interpretation of remote sensing imagery, field investigation, and literature review. Based on this dataset, we assessed the influence of different factors on the runout distance and developed prediction models of the channelized rock avalanches using the multivariate regression method. The results suggested that the movement of channelized rock avalanche was dominated by the landslide volume, total relief, and channel gradient. The performance of both models was then tested with an independent validation dataset of 8 rock avalanches that induced by the 2008 Wenchuan, the Ms7.0 Lushan earthquake, and heavy rainfall in 2013, showing acceptable good prediction results. Therefore, the travel distance prediction models for channelized rock avalanches constructed in this study is applicable and reliable for predicting the run out of similar rock avalanches in other regions.

Keywords: channelized rock avalanches; travel distance; empirical prediction; multivariate regression model; Wenchuan earthquake

1 Introduction

Rock avalanches are extremely rapid, massive flow-like movements of fragmented rock from a very large rock slide or rock fall (Hungr et al. 2014). Hundreds of rapid and long run-out rock avalanches were triggered by 2008 Wenchuan earthquake in Sichuan Province (Zhang et al. 2013), with

catastrophic consequences for residents in the affected areas. For instance, the 1.5×10^7 m^3 Donghekou rock avalanche in Qingchuan County, near the seismogenic fault, traveled 2.4 km, killing about 780 persons and destroying four villages (Zhang et al. 2013). Rock avalanches can cause incredible damage due to their characteristics of high-speed and unexpectedly long runout, while their transport mechanisms are still considered to be controversial among many researchers (Hungr et al. 2001). Therefore, constructing prediction models for rock avalanche travel distance is meaningful in terms of not only theoretical research on motion mechanisms but also in practical application for mitigation of rock avalanche risk.

Methods for determining the travel distance of landslides can be divided into two categories: dynamic modeling (Heim 1932; Hungr et al. 2009; Lo et al. 2011; Pastor et al. 2009; Sassa 1988), and empirical modeling (Scheidegger 1973; Lied et al 1980; Finlay et al. 1999; Westen et al. 2006;Guo et al. 2014). The dynamic models provide information on landslide intensity, such as velocity, affected area and deposition depth, in addition to travel distance. Nonetheless, dynamic models require accurately quantified input parameters that are difficult to obtain before the events, and many simplified assumptions that are not applicable to the actual situation. Empirical models considering the correlations between observational data provide an effective technique to aid in understanding mechanisms of rock-avalanche motion and to develop practical models for predicting rock-avalanche travel distance. However, the empirical-statistical models set up from samples with different geomorphological and geological surroundings, trigger conditions, or failure modes are not very sufficient to be applied to Wenchuan earthquake area.

In this study, we compiled a dataset of 38 rock avalanches with flow paths confined by channels (this kind of landslide is hereinafter termed as channelized rock avalanche) from interpretation of remote sensing, field investigations and literature review (see Section 3.1). Statistical correlations were used to determine the principle factors affecting the mobility of the channelized rock avalanches. Then a stepwise multivariate regression model was developed to build a best-fit empirical model for the travel-distance prediction of this kind of rock avalanches in the Wenchuan earthquake area. A derivative multivariate regression model was also constructed. The performance of both models was then tested with an independent validation dataset of 8 rock avalanches in the same area.

2 Rock avalanches in study area

The study area (see Figure 1) is on the northeast-trending Longmenshan thrust fault zone between the Sichuan basin and the Tibetan plateau. Three major sub-parallel faults are: the Wenchuan-Maowen fault, the Yingxiu-Beichuan fault and the Pengguan fault （Fan et al., 2014）With highly developed stream systems, this region is characterized by high mountains and deep valleys and extreme rates of erosion (Fu et al 2009; Qi et al 2011).

This study selected 38 channelized rock avalanches induced by the Wenchuan earthquake to study the relations between travel distance and influential factors. These rock avalanches occurred along the seismogenic Yingxiu-Beichuan fault; the distance to the fault ranged from 0 m ~21,300 m with a mean value of 3,895 m. Another distribution characteristic was is that these rock avalanches mainly clustered on the step-overs, bends and distal ends of the seismogenic fault. These distribution characteristics of the large rock avalanches suggested that the occurrence of rock avalanches was associated with very strong earthquake ground motion. The Wolong Station recorded the highest seismic acceleration with the peak ground acceleration reaching 0.948g vertically and 0.958g horizontally (Yu et al., 2009). Locally, the ground motion was high enough to throw rocks into the air.

The lithology of outcropping rock in source areas can be divided to four types: carbonaterock, phyllite, igneous rock and sandstone. The landslide deposit of the rock avalanches in the study area structure was is usually debris, which suggests that the sliding masses were intensively fragmented during their movement.

The influence of the local geomorphology on the paths of the rock avalanches was obtained from remote-sensing images after the events. Although the rock avalanches we chose all had flow paths confined by channels, some topographic differences were found to be significant in affecting present that had affected the shape morphology of the rock avalanche deposits. The source areas had well-defined boundaries. When the source mass was detached from the slide bedbedrock, it may directly move into the channel down slope (see Figure 2b), or access the channel with enter it at some impact transition angle of movement direction (see Figure 2a). The channel itself may have changes in direction and inclination. The distal end of the landslide may lie stop in the channel (see Figure 2a) or may reach to wide valley or plain (see Figure 2b).

The study area (see Figure 1) is on the northeast-trending Longmenshan thrust fault zone between the Sichuan basin and the Tibetan plateau. Three major sub-parallel faults are: the Wenchuan-Maowen fault, the Yingxiu-Beichuan fault and the Pengguan fault （Fan et al., 2014）. With highly developed stream systems, this region is characterized by high mountains and deep valleys and extreme rates of erosion (Fu et al 2009; Qi et al 2011).

This study selected 38 channelized rock avalanches induced by the Wenchuan earthquake to study the relations between travel distance and influential factors. These rock avalanches occurred along the seismogenic Yingxiu-Beichuan fault; the distance to the fault ranged from 0 m ~21,300 m with a mean value of 3,895 m. Another distribution characteristic is that these rock avalanches mainly clustered on the step-overs, bends and distal ends of the seismogenic fault. These distribution characteristics of the large rock avalanches suggested that the occurrence of rock avalanches was associated with very strong earthquake ground motion. The Wolong Station recorded the highest seismic acceleration with the peak ground acceleration reaching 0.948g vertically and 0.958g horizontally (Yu et al., 2009). Locally, the ground motion was high enough to throw rocks into the air.

The lithology of outcropping rock in source areas can be divided to four types: carbonaterock, phyllite, igneous rock and sandstone. The deposit of the rock avalanches in the study area is usually debris, which suggests that the sliding masses were intensively fragmented during their movement.

The influence of the local geomorphology on the paths of the rock avalanches was obtained from remote-sensing images after the events. Although the rock avalanches we chose all had flow paths confined by channels, some topographic differences were found to be significant in affecting the morphology of the rock avalanche deposits. When the source mass was detached from the bedrock, it may directly move into the channel down slope (see Figure 2b), or enter the channel with some transition angle of movement direction (see Figure 2a). The channel itself may have changes in direction and inclination. The distal end of the landslide may stop in the channel (see Figure 2a) or may reach to wide valley or plain (see Figure 2b).

3 Data and method

3.1 General consideration

Various statistical methods have been applied to predict travel distance of landslides. The most prevalent one is the equivalent friction coefficient model, which only takes account of landslide volume (Scheidegger 1973). Another well-known model is the statistical α–β model in which the maximum runout distance is solely a function of geography (Lied et al., 1980; Gauer et al., 2010). Finlay et al.(1999) developed some multiple regression models containing slope geometric parameters like slope height and slope angle for the travel distance prediction of landslides on the artificial slopes upon the horizontal surface. Based on the data of 54 landslides which was relatively open or confined by gentle lateral slope, Guo et al.(2014) established an empirical model for predicting landslide travel distance in Wenchuan earthquake area and suggested that rock type, landslide volume, and slope transition angle play dominant roles on landslide travel distance. And there are increasing sound that the prediction models of travel distance should adapt to different types of landslides (Corominas 1996; Fan et al, 2014;).

Moreover, the local morphology plays an important role on shape and mobility of rock avalanches. Heim (1932) firstly mentioned the influence of local morphology that the debris masses will undergo different effects with the angle of impact changing, and rock avalanches has to conform to the local morphology regardless of their scale. Abele (1974) summarized four different possibilities of adaptation of the rock avalanche to local morphology. Hsu(1975) noted that a sinuous pathway can reduced runout distance of rock avalanches. Nicoletti (1991) inferred that local morphology impacts on landslide motion through changing the rate of total energy dissipation along the travel path. To determine the influence of specific channels on the travel distances of rock avalanches, we respectively consider the impacts of gradients of the upper slopes and lower channels.

Rock avalanches triggered by Wenchuan earthquake usually initiated from top or the higher part of slopes possibly due to the altitude amplification effect of earthquake acceleration, therefore the toe of the rupture surface is commonly found in the source area at the upstream of the channel (See Figure 3). When the slope failed, the failed mass travelled a long distance down the channel. The 38 rock avalanches in this study are selected with the criterion that the flow path is partially or fully confined by channels. The volumes of these rock avalanches ranged from 0.4–50×$10^6$$m^3$; with horizontal travel

distances between 0.58 and 4.00 km. The volume is prior to the area to be put into the travel distance prediction model as it had much more physical meanings. And we introduced total relief as well as the height of source area to probe the influences of the potential energy difference and altitude difference of source mass on the travel distance of the rock avalanches.

3.2 Data

The terms and notations of a typical channelized rock avalanche are shown in Figure 3. The local morphology of a rock avalanche can be divided to three sections: initiated slope (source area), channel (main travel path or flow area) and valley floor (deposition area). When the mass moves over the slope section, it is free from lateral constraints, and the moving mass is able to spread laterally. After entering the channel, the flowing mass is constrained by the two lateral slopes. Finally, the mass may reach to a wide valley floor, where it spreads laterally and deposits. The average inclination of slope section and valley section are obtained respectively, while the gradient of valley section is neglected as it has very little variation. Slope angle（α）, denotes the average inclination of the initiated slope section. Channel angle（β）, denotes the average inclination of the sectional channel. Source area height (Hs), denotes the elevation difference between the crest of the sliding source and the toe of the rupture surface. Total relief (H) is the elevation difference between the crest of the sliding source and the distal end of the debris deposit. Travel distance (L) is the horizontal distance between the crest of the sliding source and the distal end of the debris deposit. Landslide area (A) is the source area of the rock avalanche obtained from remote sensing image interpretation. An empirical scaling relationship with different empirical coefficients is frequently used to link the volume and the area of landslides in different areas or with different types, and we chose the one developed by Parker et al. (2011) in the same study area. Volume of some rock avalanches with detailed field investigation are replaced by the data from published literature. The parameters of 38 rock avalanches are listed in Table 1.

3.3 Method

Travel distance is the most desired prediction in rock-avalanche hazard evaluation in mountainous areas. Travel distance prediction of rock avalanche is a complicated issue as it is determined by many different properties of the materials (i.e., grain size distribution and water content), topographical factors, mobility mechanics of failed mass, the confinement attributes of travel path, and so on (Guo et

al., 2014). Empirical-statistical methods have long been used as tools to study the mobility of rock avalanche since they are easy to develop and apply, and they are not dependent on knowing the physical processes involved in causing the mobility. Channelized rock avalanches have unique movement paths involving complex, and possibly little-known physical processes such as grain collisions, fragmentation and entrainment of bed material from the channel sides and bottom. Existing empirical models have not produced a favourable prediction. The forecasting index system and the prediction model of channelized rock avalanches should be discussed first.

In this paper, we first selected controlling factors on rock avalanche travel distance through correlation analysis. Then we fitted a stepwise multivariate regression model using all significant correlation variables to obtain a best-fit empirical model for landslide travel distance, and explored which factors were statistically significant at the same time, as expressed in equation (1).

$$y = b_0 + b_1 x_1 + b_2 x_2 + b_3 x_3 + ... + b_n x_n + \varepsilon \qquad (1)$$

where y is the predictant ('dependent variable'), e.g. travel distance of rock avalanche, (i = 1, 2, …, n) are the predictors ('independent variables'), b_0 is the intercept, (i= 1, 2, …, n) are the regression coefficients of the corresponding , and ε is the residual error, here assumed to be independently and normally distributed. Predictors were added to the regression equation one at a time until there was no significant improvement in parsimonious fit as determined by the adjusted R^2.

4 Results and validation

4.1 Relationships between travel distance and volume, topographic relief of rock avalanche

Correlation coefficients between different variables and travel distance (L) were calculated first, generating the correlation coefficients matrix shown in Table 2. The significant relevant predictors with the 95% confidence for travel distance prediction of channelized rock avalanche are landslide area(A), landslide volume(V), total relief(H), source area height(Hs), and channel angle(β), with correlation coefficient of 0.877, 0.866, 0.857, 0.675, -0.467, respectively.

Figures 4 illustrates that the travel distance (L) varies exponentially with volume (V) of rock avalanche with an exponential exponent of 0.377. Compared with a compilation of world-wide rock-avalanche data (Legros, 2002), the mobility of rock avalanches in our study area is stronger than other non-volcanic landslides (power exponent is 0.25), but weaker than volcanic landslides and debris flows

(both power exponent is 0.39). The relation between travel distance (L) and total relief (H) is shown in figure 5. The result suggests that the mobility (travel distance) of rock avalanche has relatively strong linear relationship with total relief (H). The scale factor is close to 2.4, which means that the apparent friction coefficient (H/L) for the rock avalanches is approximately 0.42. This is significantly lower than the commonly observed static coefficient of friction of rock material (~0.6).

4.2 Multivariate regression model of rock avalanche travel distance

According to the matrix of correlation coefficients (Table 2), the slope angle (α) does not have a significant correlation with travel distance (L) at the 95% confidence level. Thus this variable could be excluded first during development of the best-fit regression model for travel distance prediction. Prior to the landslide area (A), the landslide volume (V) has been considered in the models as it has much more physical meaning. In the end, a stepwise linear multivariate regression technique was applied to find the best-fit travel distance regression model using the significant relevant predictors including landslide volume (V), total relief (H), source area height (Hs) and channel angle (β). The best-fit regression equation for travel distance prediction were derived from the dataset of Table 1 (see equation (2)), and the coefficient of the variables with 95% confidence are shown in Table 3.

$$\log(L) = 0.420 + 0.079\log(V) + 0.718\log(H) - 0.365\log(\tan\beta) \qquad (2)$$

Where log is the logarithm of 10; L is the predicted travel distance (m); V is the landslide volume (m^3); H is the total relief (m); β is the mean gradient of the channel (°).

Equation (2) can be transformed to equation (3):

$$L = 2.630\,V^{0.079}H^{0.718}(\tan\beta)^{-0.365} \qquad (3)$$

The best-fit travel distance regression equation indicates that the travel distance of channelized rock avalanche is positively correlated with landslide scale (landslide volume) and potential energy loss(total relief), and negatively correlated with channel gradient(channel angle),which is coherent with the results of correlation analysis in table 2.

While the total relief (H) will be unknown prior to landslide occurrence, the elevation difference of source area will be available through specific field investigation on a potential rock avalanche area. Hence, we introduced Hs and α in replacement of H to the regression model as they have relative high correlation with H (correlation coefficients are 0.801 and 0.429 respectively). The transformed

alternative regression equation is given as equation (4) with the coefficient of the variables with 95% confidence in table 3.

$$L = 3.6V^{0.303}Hs^{0.244}(\tan\alpha)^{-0.115}(\tan\beta)^{0.072} \quad (4)$$

Where L is the predicted travel distance (m); V is the landslide volume (m^3); Hs is the height of source area (m); α is the mean angle of slope segment (°); β is the mean gradient of the channel segment (°).

The validity of these two models were evaluated through the significance test leading to the highest R^2 value and the lowest residual standard error. Table 3 shows the significance values for the prediction model equations. Adjusted R^2 means adjusted multiple correlation coefficient, which represents the correlation level between the dependent variable and the independent variables. The calculation of adjusted R^2 considers the number of variables and can be used to compare goodness of fit of different regression models. Adjusted R^2 of the two regression equations are high, suggesting that the constructed regression models are reliable. The adjusted R^2 of equation (4) is higher than equation (5), implying a higher precision for the best-fit regression model. The significance test results on the regression equation suggest the significance of multiple regression equations (($F=173.5 > F_{0.05}(2.883)$ for equation(2) and $F=49.5 > F_{0.05}(2.659)$ for equation (4)). Figures 6 and 7 show the distributions of the residuals in relation to the observed travel distance estimated by using equation (2) and (4). Both plots illustrates normality, constant variance and absence of trends in the residuals.

Figure 8 compares the predicted travel distances estimated by using equations (2) and (4) with the observed ones. It suggests that the predicted values of the samples are close to the observed ones. Where L exceeds 2000 m, the predicted travel distance calculated by using two models are lower than actual one, with relatively large residual error. The largest residual error appears in Wenjia gully rock avalanche, followed by Hongshi Gully, Niumian Gully and Donghekou rock avalanche. According to the field investigation, projectile motion was experienced for these four rock avalanches with vertical drop of 260 m, 150 m, 60 m and 160 m respectively before they flowed along the channel downslope. Moreover, fluidization characteristics such as super-elevation near curve transitions can be found in the channel section of these four rock avalanches. These findings manifest the steep micro-geotopography will enlarge the mobility of rock avalanches as this kind of topography will lead the slide mass to undergo the projection, collision, fragmentation effects in the early motion stage which will facilitate

motion mode transformation from sliding to flowing. This transformation will enhance the motion mobility of rock avalanche to travel a much longer distance than predicted one.

4.3 Validation

The regression equations were tested using an independent sample validation data set （Table 4）of 8 rock avalanches in the same area induced by three different kinds of triggers: 2008 M_s7.8 Wenchuan earthquake, 2013 M_s7.0 Lushan earthquake, and heavy rainfall. The volume of these samples ranged from 8.8×10^4–$150\times10^4 m^3$, and travel distance from 372–1372 m. The background parameters and the predicted values of each avalanche are listed in Table 4. The relative errors between the predicted values estimated by using equation (3) and observed values of the travel distance of the rock avalanches, $|L_{predicted}-L_{observed}|/L_{observed}\times100\%$, are between -14.4% and 17.2%, while the relative errors are -44.0% and 17.9% for equation (4). On the whole, these two regression models achieved acceptable prediction accuracy for preliminary forecasting of travel distance of rock avalanches in rugged mountainous areas. The best-fit regression model appeared to provide greater precision than the alternative model. Regarding the influence of triggers on the travel distance of the channelized rock avalanches, those triggered by rainfall and the Lushan earthquake seemed to be more mobile. It is inferred that the former difference is due to the high water content in failed mass induced by rainfall. A possible reason why two rock avalanches triggered in the Lushan earthquake travelled farther may be because of structural weakening of slope rock mass in the 2008 Wenchuan earthquake in the study area.

5 Discussion

5.1 Prediction for travel distance of channelized rock avalanche

The results of our analysis of the data set, indicates that the mobility (travel distance) of channelized rock avalanche is positively correlated with landslide volume and total relief but negatively correlated with channel angle. It is inferred that the movement of channelized rock avalanche was strictly constrained by the local geomorphology. As Figure 3 shows, the travel distance of channelized rock avalanche would rapidly increase with volume of rock avalanche enlarged. Such a high correlation between landslide volume and travel distance implies that the travel distance of channelized rock avalanche is dominated by the spreading of the slide mass (Davies, 1982; Staron,2009). The high

positive correlation between total relief and travel distance is for two reasons: the larger the total relief is, the more kinetic energy the slide mass could obtained and the further distance could it travel; another contribution is the geometrical similarity of hillslope geomorphology in the study area (Legros, 2002).

Regarding the medium negative correlation between travel distance and channel angle, it is inferred that when the slide mass rushed into the channel after the acceleration movement on the upper hillslope, it had relatively high velocity and extremely low frictional coefficient among the rock fragments, and the channel could not stop the rock avalanche until it lost fragment flow discharge. Hence, the travel distance of channelized rock avalanche would increase with the channel angle cut down given the same flow discharge (landslide volume), relative stable flow velocity, and similar flow capacity. However, it is still difficult to evaluate the flow capacity of the channels due to difficulty of quantifying its cross-section shape (width and depth of channels), resistance to the rock avalanche and even the shape changing induced by entrainment process of rock avalanche.

The residual analysis result demonstrates that the projection process in the early motion stage will significantly enlarge the travel distance of rock avalanches. The nature of this phenomenon is suggested to be involved with transformation of motion mode from sliding to flowing due to collision and fragmentation effects after the projection (Davies et al, 1999). Furthermore, the degree of fragmentation of failed mass should have remarkable influence on the travel distance of rock avalanche, and other factors changing the fragmentation degree should be further study, such as earthquake effect, geologic structure and rock type.

5.2 Conceptual model for transportation of channelized rock avalanche

The statistical results imply that the travel distance of channelized rock avalanche is highly correlated with landslide volume, total relief and channel angle. As the total relief and channel angle act as external factors for the motion of rock avalanche, it seems like it is in essence landslide volume that control the rock avalanche movement. Actually, a good fitting result between travel distance and landslide volume appears on our data set (Figure 4). So we propose a conceptual model for channelized rock avalanche transportation: An initial failed mass rushes into the channel with certain velocity after acceleration and fragmentation effects over the upper slope. Then the failed mass will “forget” the initial fall height and flow down in the channel like unsteady flow. The flow discharge (including

initial landslide volume and entrainment volume) and the flow capacity of the channel control the travel distance of channelized rock avalanche without considering the motion mechanism.

However, the flow capacity varies along the channel. Some local depression can store a mass of the moving rock debris, causing a lack of flow discharge for the downstream channel and a considerable decrease of travel distance. Taking Wenjia Gully rock avalanche for an example, almost a half of total volume of the landslide deposit on the beginning of the channel (red dash circle area in Figure 9), leading to that the distal deposition appeared in the channel instead of the valley. Thus assessing the flow capacity of the channel for rock avalanche motion will assist in future forecast of potential rock avalanche hazard in mountainous areas.

6 Conclusion

Channelized rock avalanche refers to a rock avalanche with a flow path confined between valley walls. Relevant Detailed data on thirty-eight channelized rock avalanches triggered by Wenchuan earthquake were collected by remote sensing, field investigation and literature review. The results of correlation and regression analysis revealed that the movement of channelized rock avalanches is dominated by spreading of the failed mass. Landslide volume (V), total relief (H) and channel angle (β) had predominant effects played a dominating role in the on travel distance of channelized rock avalanches. Stepwise multivariate regression was used to develop a nonlinear best-fit travel distance prediction model for the channelized rock avalanches. An alternative multivariate regression model was also built. The reliability of the two models was tested on by an independent validation dataset of 8 rock avalanches in the same area and produced good results, meeting the requirements for preliminary evaluation of travel distance for channelized rock avalanches in the Wenchuan earthquake area.

Acknowledgement

This work was supported by the Young Scientists Fund of the National Natural Science Foundation of China (Grant No. 41302241), the Fund for Creative Research Groups of China (Grant No. 41521002), the Fund for International Cooperation (NSFC-RCUK_NERC), Resilience to Earthquake-induced landslide risk in China (Grant No. 41661134010). The authors thank Dr. Mauri McSaveney for his constructive comments and editing the English the paper.

References

Davies, T. R., McSaveney, M. J., and Hodgson, K. A.: A fragmentation-spreading model for long-runout rock avalanches, Canadian Geotechnical Journal, 36, 1096-1110, 1999.

Fan, X., Rossiter, D. G., Westen, C. J., Xu, Q., and Görüm, T.: Empirical prediction of coseismic landslide dam formation, Earth Surface Processes and Landforms, 39, 1913-1926, 2014.

Finlay, P. J., Mostyn, G. R., and Fell, R.: Landslide risk assessment: prediction of travel distance, Canadian Geotechnical Journal, 36, 556-562,1999.

Guo, D., Hamada, M., He, C., Wang, Y., and Zou, Y.: An empirical model for landslide travel distance prediction in Wenchuan earthquake area, Landslides, 11, 281-291, 2014.

Heim, A.: Bergsturz und menschenleben (No. 20), Fretz and Wasmuth, 1992.

Hungr, O., Evans, S. G., Bovis, M. J., and Hutchinson, J. N.: A review of the classification of landslides of the flow type, Environmental and Engineering Geoscience, 7, 221-238, 2001.

Hungr, O., and McDougall, S.: Two numerical models for landslide dynamic analysis, Computers and Geosciences, 35, 978-992, 2009.

Hungr, O., Leroueil, S., and Picarelli, L.: The Varnes classification of landslide types, an update, Landslides, 11, 167-194, 2014.

Hsü K J.: Catastrophic debris streams (sturzstroms) generated by rockfalls, Geological Society of America Bulletin, 86, 129-140, 1975.

Legros, F.: The mobility of long-runout landslides, Engineering Geology, 63, 301-331, 2002.

Lied, K., and Bakkehøi, S.: Empirical calculations of snow-avalanche run-out distance based on topographic parameters, Journal of Glaciology, 26, 165-177, 1980.

Lo, C. M., Lin, M. L., Tang, C. L., and Hu, J. C.: A kinematic model of the Hsiaolin landslide calibrated to the morphology of the landslide deposit. Engineering Geology, 123, 22-39, 2011.

Nicoletti, P. G., and Sorriso-Valvo, M.: Geomorphic controls of the shape and mobility of rock avalanches, Geological Society of America Bulletin, 103, 1365-1373, 1991.

Parker, R. N., Densmore, A. L., Rosser, N. J., De Michele, M., Li, Y., Huang, R., ... and Petley, D. N: Mass wasting triggered by the 2008 Wenchuan earthquake is greater than orogenic growth, Nature Geoscience, 4, 449-452, 2011.

Pastor, M., Haddad, B., Sorbino, G., Cuomo, S., and Drempetic, V.: A depth‐integrated, coupled SPH model for flow‐like landslides and related phenomena, International Journal for numerical and analytical methods in geomechanics, 33, 143-172, 2009.

Qi, S., Xu, Q., Zhang, B., Zhou, Y., Lan, H., and Li, L.: Source characteristics of long runout rock avalanches triggered by the 2008 Wenchuan earthquake, China, Journal of Asian Earth Sciences, 40, 896-906, 2011.

Sassa, K.: Geotechnical model for the motion of landslides, In: AA Balkema (ed.) Proceedings of the 5th International Symposium on Landslide, Rotterdam, 37-55, 1988.

Scheidegger, A. E.: On the prediction of the reach and velocity of catastrophic landslides, Rock Mechanics and Rock Engineering, 5, 231-236, 1973.

Staron, L., and Lajeunesse, E.: Understanding how volume affects the mobility of dry debris flows, Geophysical Research Letters, 36, 2009.

Van Westen, C. J., Van Asch, T. W., and Soeters, R.: Landslide hazard and risk zonation—why is it still so difficult?, Bulletin of Engineering geology and the Environment, 65, 167-184, 2006.

Xu, Q., Pei, X. J., and Huang, R. Q.: Large-scale landslides induced by the Wenchuan earthquake. Science, Beijing, 2009 (In Chinese).

Yu, H., Wang, D, Yang, Y., Xie, Q., Jiang, W., and Zhou, B.: The preliminary analysis of strong ground motion records from the M_s 8.0 Wenchuan Earthquake, Journal of Earthquake Engineering and Engineering Vibration, 1, 000, 2009.

Zhang, M., and Yin, Y.: Dynamics, mobility-controlling factors and transport mechanisms of rapid long-runout rock avalanches in China, Engineering Geology, 167, 37-58, 2013.

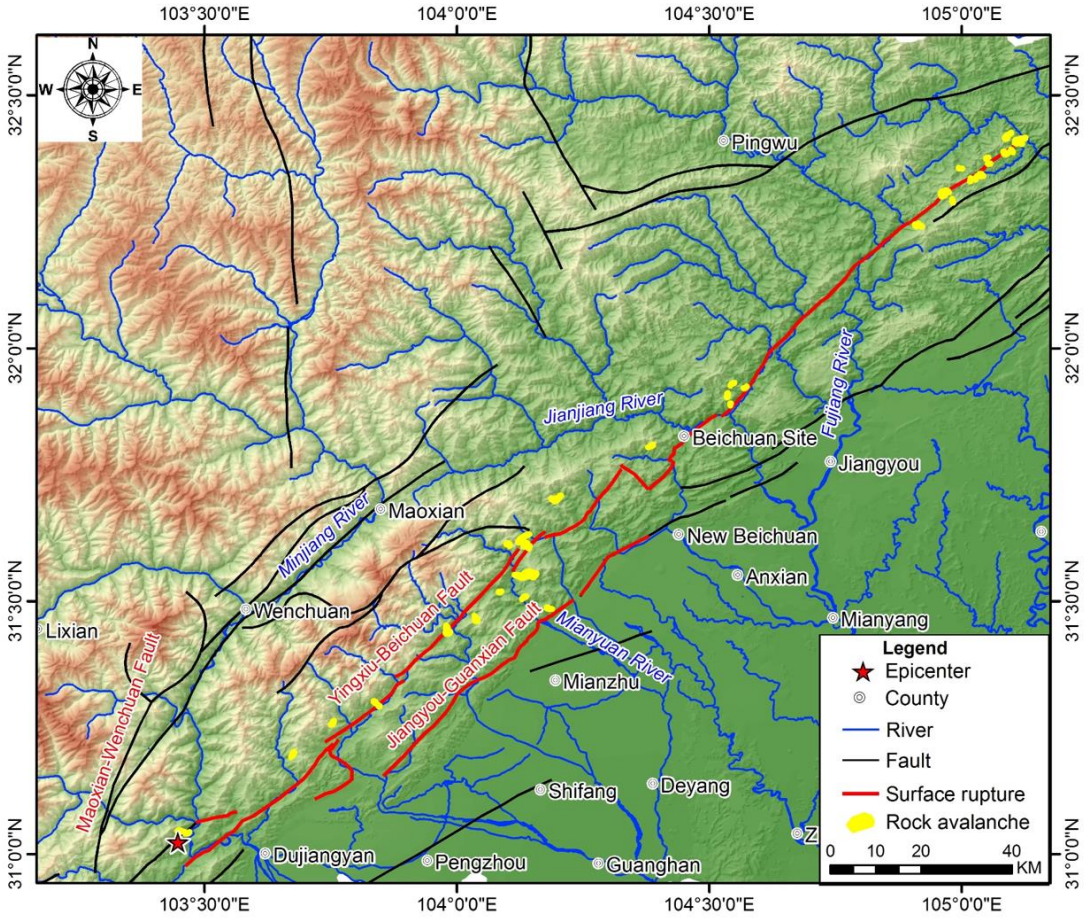

391

392 **Figure 1: Distribution map of large rock avalanches triggered by the Wenchuan earthquake.**

393

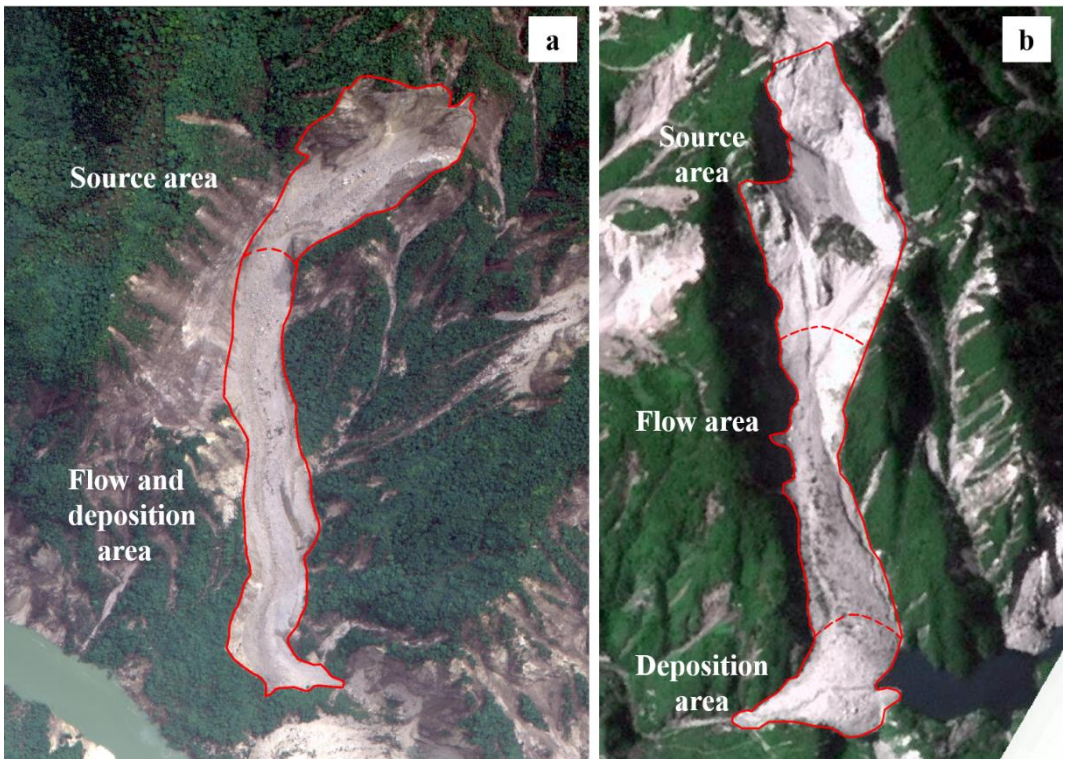

394

Figure 2: Remote-sensing images of two channelized rock avalanches triggered by the Wenchuan earthquake. a is Changtan rock avalanche (No.21 in table 1); b is Laoyingyan rock avalanche, which is river-blocked.

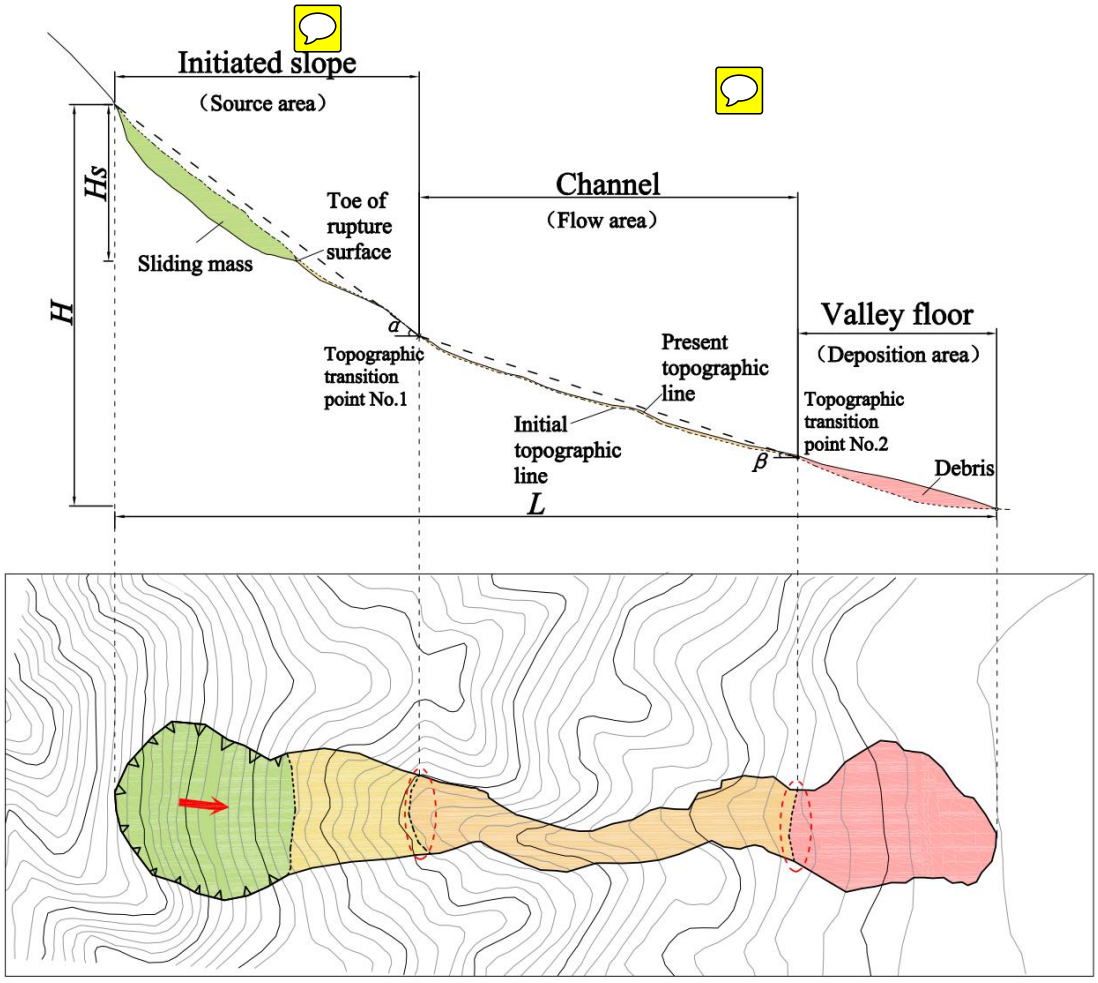

Figure 3: Sketch map of a channelized rock avalanche defining geometric parameters. The red-dashed ellipse indicates the topographic transition dividing the initiated slope, channel and valley floor. The red arrow represents sliding direction of source mass.

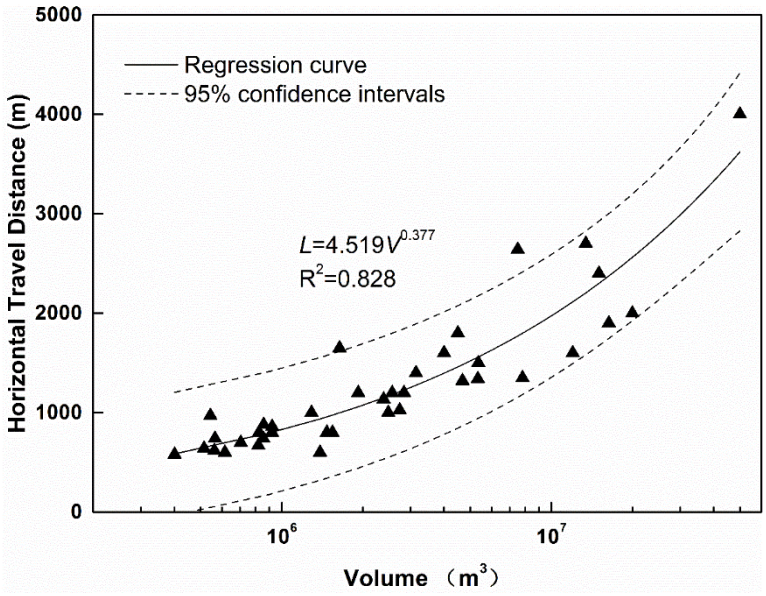

402 **Figure 4: Relationship between horizontal travel distance and volume of channelized rock avalanches.**

403

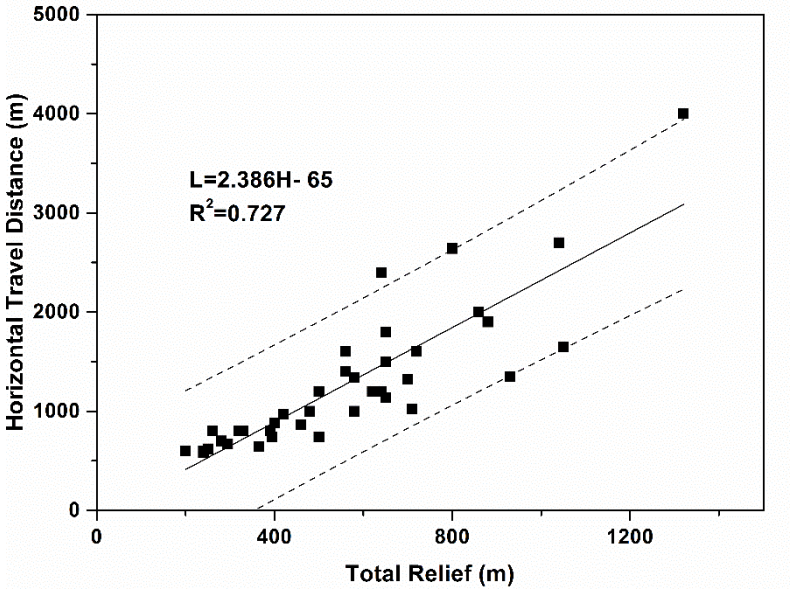

Figure 5: Relationship between horizontal travel distance and total relief of channelized rock avalanche.

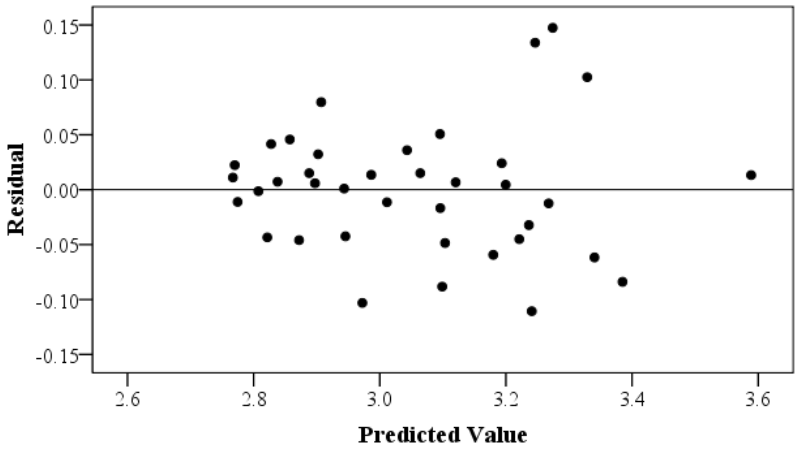

Figure 6: Residual plot for equation (2).

404

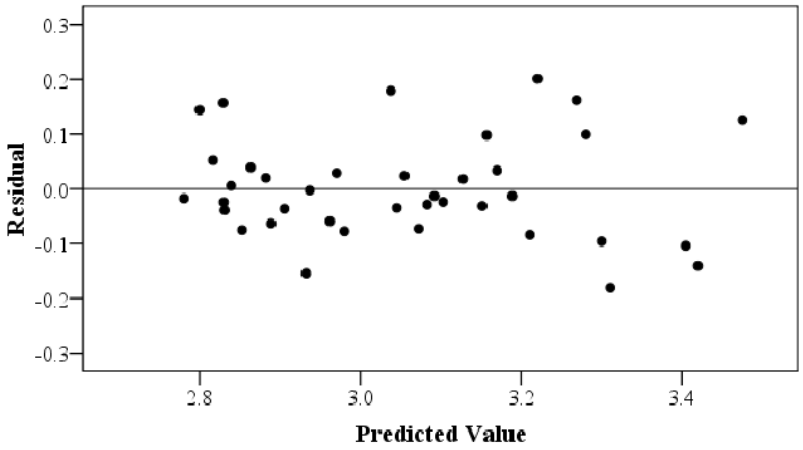

Figure 7: Residual plot for equation (4).

405

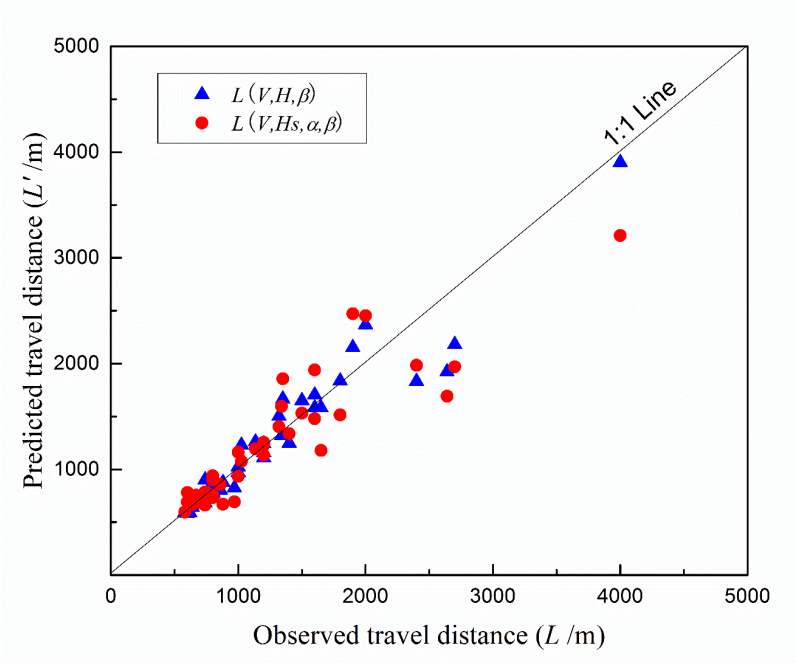

Figure 8: The comparison between observed and predicted travel distance for the two multivariate regression models.

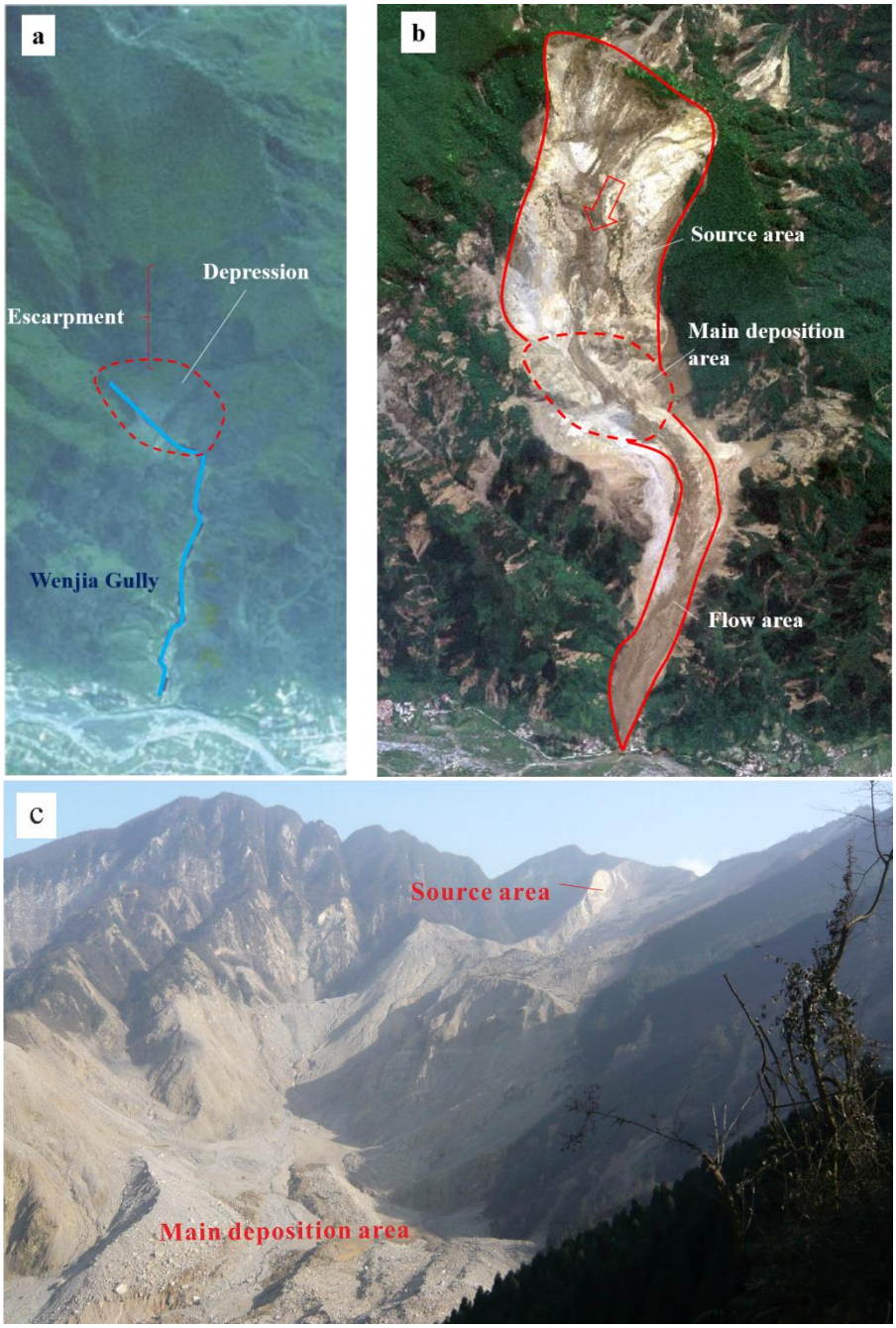

406

407 **Figure 9: Sketch map of flow capacity of channel affecting on the travel distance of Wenjia Gully**
408 **channelized rock avalanche: (a) before the earthquake, (b) after the earthquake, (c) photo taken on**
409 **deposition platform after the earthquake. The red arrow show the sliding direction of source mass. The red**
410 **dotted line in figure.9(a) indicates the original depression on the travel path of the rock avalanche, in where**
411 **debris deposition of about 30 million m3 was stored after the earthquake (shown in figure.9(b)), and more**
412 **detailed information is shown in the figure.9(c).**

413

Table 1: Data of various factors for establishment of prediction model of rock avalanche travel distance.

Code	Landslide name	Longitude, (°E)	Latitude, (°N)	Landslide area, A (m^2)	Landslide volume, V (m^3)	Source area height, Hs (m)	Slope angle, α (°)	Channel angle, β (°)	Total relief, H (m)	Travel distance, L (m)	Reference
1	Wenjia Gully	104.140	31.552	3000566	50000000	440	26	7	1320	4000	Xu et al., 2009
2	Shuimo Gully	103.981	31.442	915608	19960000	490	35	10	860	2000	
3	Dawuji	104.196	31.702	792190	16330000	540	29	13	880	1900	
4	Donghekou	105.113	32.410	1283627	15000000	240	25	11	640	2400	Xu et al., 2009
5	Hongshigou	104.130	31.624	687520	13410000	290	37	17	1040	2700	
6	Woqian	104.964	32.308	695672	12000000	330	30	10	560	1600	Xu et al., 2009
7	Xiaojiashan	104.038	31.465	465899	7810000	480	48	24	930	1350	
8	Niumian Gully	103.456	31.044	527700	7500000	320	32	13	800	2640	Xu et al., 2009
9	Liqi Gully	105.207	32.169	355113	5360000	360	37	12	650	1500	
10	Caocaoping	104.139	31.607	354046	5340000	345	31	17	580	1340	
11	Huoshi Gully	104.134	31.616	322155	4680000	270	38	17	700	1320	
12	Shibangou	105.090	32.419	496983	4500000	450	34	9	650	1800	Xu et al., 2009
13	Xiejiadianzi	103.841	31.298	294256	4000000	400	34	15	720	1600	Xu et al., 2009
14	Dashui Gully	103.675	31.199	241874	3150000	320	30	17	560	1400	
15	Changping	103.754	31.259	224645	2840000	290	37	16	500	1200	
16	Xiaomuling	104.102	31.613	218704	2740000	175	45	26	710	1025	
17	Baishuling	104.385	31.807	208968	2570000	335	36	20	620	1200	
18	Dawan	104.536	31.907	203959	2480000	220	28	20	480	1000	
19	Xiaojiashan	104.182	31.486	198165	2385499	340	44	20	650	1135	
20	Shicouzi	104.918	32.243	169540	1920000	260	30	26	640	1200	

21	Changtan	104.133	31.508	151094	1640000	400	33	25	1050	1650
22	Hongmagong	104.962	32.301	144683	1540000	195	30	14	330	800
23	Baiguocun	105.088	32.385	139800	1470000	165	26	12	260	800
24	Qinglongcun	105.036	32.342	134079	1390000	90	21	11	200	600
25	Pengjiashan	104.546	31.930	127156	1290000	200	33	28	580	1000
26	Longwancun	104.571	31.922	99821	920000	205	31	28	460	860
27	Zhangzhengbo	105.017	32.333	99726	920000	125	29	15	320	800
28	Dujiayan	105.028	32.336	94769	860000	100	33	17	400	880
29	Madiping	104.996	32.355	94632	860000	140	27	31	395	740
30	Yandiaowo	105.099	32.391	92128	820000	145	30	26	390	800
31	Chuangzi Gully	104.085	31.518	91717	820000	185	35	15	295	670
32	Zhaojiashan	105.041	32.342	82329	700000	115	22	16	280	700
33	Weiziping	105.083	32.387	74661	620000	135	22	18	240	600
34	Maochongshan 2	104.908	32.243	70251	570000	160	38	22	500	740
35	Waqianshan	105.049	32.376	70007	560000	135	24	18	250	620
36	Muhongping	104.982	32.291	68288	540000	175	28	20	420	970
37	Dapingshang	104.542	31.889	65700	520000	160	34	29	365	640
38	Liushuping 2	105.054	32.365	54810	400000	150	29	16	240	580

Table 2: Correlation coefficients of continuous variables listed in Table 1.

	A	V	H	Hs	*α*	*β*	L
A	1.000	0.982	0.674	0.521	*-0.119*	-0.524	0.877
V	—	1.000	0.713	0.560	*-0.055*	-0.492	0.866
H	—	—	1.000	0.801	0.429	*-0.130*	0.857
Hs	—	—	—	1.000	0.399	-0.323	0.675
α	—	—	—	—	1.000	*0.264*	*0.082*
β	—	—	—	—	—	1.000	-0.467
L	—	—	—	—	—	—	1.000

Note: The number in Italics indicates the two variables are not significantly correlated

Table 3: The regression coefficients and results of significance tests of two multivariate regression models.

Equations	Coefficients*	Intercept	Coefficient of log(V)	Coefficient of log(H)	Coefficient of log(tan*β*)	Coefficient of log(Hs)	Coefficient of log(tan*β*)	Adjusted R^2	F_{stat}	$F_{0.05}$
Best-fit regression equation	LCI	0.175	-0.013	0.521	-0.548	—	—	0.933	173.5	2.883
	Mean	0.420	0.079	0.718	-0.365	—	—			
	UCI	0.665	0.171	0.914	-0.182	—	—			
Alternative regression equation	LCI	0.110	0.199	—	-0.165	-0.002	-0.464	0.840	49.5	2.659
	Mean	0.561	0.303	—	0.072	0.244	-0.115			
	UCI	1.012	0.407	—	0.308	0.489	0.233			

Note: "Coefficients" of each variable has three kinds: LCI is lower bound of the coefficients with 95% confidence; Mean is the mean value of the coefficients; UCI is upper bound of the coefficients with 95% confidence;

Table 4: Background parameters and predicted values of 8 rock avalanches in the same area used for validation

Landslide name	Longitude	Latitude	Triggers*	*V* /$10^4 m^3$	*α* /°	*B* /°	*Hs* /m	*H* /m	*L* /m	$L'_{(3)}$** /m	Error / %	$L'_{(4)}$*** /m	Error / %
Pianqiaozi	104.370	31.822	WCEQ	8.8	35	19	153	205	372	436	17.2	373	0.3
Yangjiayan	104.328	31.755	WCEQ	25.4	41	23	164	304	518	583	12.5	518	0.1
Shanshulin	103.508	31.181	WCEQ	27.9	34	25	340	433	715	731	2.3	660	-7.6
Fuyangou	103.501	31.422	WCEQ	71.9	38	28	385	530	763	869	13.8	900	17.9

Dayanbeng1	102.762	30.179	LSEQ	100	53	10	254	424	1267	1136	-10.3	781	-38.4
Dayanbeng2	102.761	30.178	LSEQ	110	50	8	237	407	1372	1208	-12.0	787	-42.6
Ermanshan	102.739	29.322	RF	100	33	15	148	635	1370	1303	-4.9	767	-44.0
Wulipo	103.567	30.919	RF	150	30	10	135	377	1260	1078	-14.4	833	-33.9

Note: "Triggers" is the triggering condition of rock avalanches: "WCEQ" represents the 2008 Wenchuan Ms7.8 earthquake; "LSEQ" represents the 2013 Lushan Ms7.0 earthquake; "RF" represents the rock avalanche was induced by heavy rainfall. $L'_{(3)}$, $L'_{(4)}$ indicates the predicted travel distance estimated by using equation (3) and (4) respectively.

5